


**COVER PAGE**

***Document downloaded by @DAEL***

***Fri Nov 27 04:58:39 2026***
***For personal use***

When automatic English translation is provided, only the original document is authentic.
The EAA cannot be held responsible of any translation error

Bibliographical reference

*Data Extrapolation Method Based on Patch Near-Field Acoustic Holography*, Wen-Qiang Jia, Jin Chen, Jia-Qing Li and Chao Yang, Acta Acustica **vol. 95** (Number 1), 2009, pp. 142-150

DOI
https://doi.org/10.3813/AAA.918135

ACTA ACUSTICA UNITED WITH ACUSTICA
Vol. 95 (2009) 142 – 150

Technical and Applied Papers
DOI 10.3813/AAA.918135

# Data Extrapolation Method Based on Patch Near-Field Acoustic Holography

Wen-qiang Jia, Jin Chen, Jia-qing Li, Chao Yang
State Key Laboratory of Mechanical System and Vibration, Shanghai Jiao Tong University, Shanghai 200240, China. jiawenqiang@sjtu.edu.cn

**Summary**
Near-field acoustical holography (NAH) requires the measurement of the pressure field over a closed surface in order to recover the normal velocity on a nearby concentric surface. It is impractical for large structure when the reconstruction of the field is required only on a partial structure surface. The method of superposition may be applied to reconstruct the field on a partial surface on a structure form measurements made on a nearby limited surface. According to the wave superposition method (WSM), the field on and near the measurement surface may be approximated by the field produced by virtual source points placed on a surface inside the structure. The source strengths are evaluated by applying boundary conditions on the measurement surface. Here, an iterative procedure is applied to extend the measurement surface in order to obtain better reconstruction precision. The algorithm requires the inversion of the Green's function matrix which may be ill-conditioned. Tikhonov regularization method is used to invert it, and the value of the regularization parameter is determined based on use of the L-curve criteria. A numerical simulation of two ball sound sources as an example to validate the results is used. The result of experiment shows the superiority and applicability of the data extrapolation based on patch-NAH.

**PACS no. 43.20.Rz, 43.40.Rj, 43.50.Yw**

## 1. Introduction

Acoustical holography [1, 2] can reconstruct a three dimensional image based on the information obtained over a two dimensional holography surface. The problem is ill-posed because of the presence of evanescent waves that decay rapidly from the vibrating to the measurement surface. The measurements are typically made very close to the vibrating surface in order to obtain a high resolution reconstruction. To treat the ill-posed nature of the problem, many methods are used. When the structure has a regular surface, Fourier decomposition is used with the series truncated to remove the very short wavelength components of the field that decay very rapidly [1, 3]. For an arbitrarily shaped surface, boundary element methods may be applied to discretize the integral equation representations of the acoustical pressure in order to obtain a relation between the measurement pressure and the acoustic field over the structure surface in matrix form [4, 5, 6] The resultant matrix is also ill-posed and requires the use of regularization methods for its solution. The common implementation procedure of regularization is based on the calculation of the singular value decomposition and Tikhonov regularization[7, 8].

Conformal near-field acoustical holography demands that the measurement aperture must larger than the reconstructed sound source. However, it is impractical for large structure when the reconstruction of the field is required only on a partial structure surface. For this case, patch near-field acoustical holography [8, 9, 10, 11, 12] may be applied where measurements need to be made only on a surface that is approximately as large as the patch on the structure surface where the reconstruction is required.

The method of superposition [13, 14, 15, 16, 17] is applied which approximates the field on and near measurement surface by the superposition of fields produced by a number of sources placed on a surface near the measurement surface. The source strengths are determined by applying boundary conditions on the measurement surface. It can be used either to enlarge a finite measurement aperture or to fill in gaps within the measurement aperture. Here we apply data extrapolation method based on wave superposition with Tikhonov regularization to reconstruct the sound field in patch holography. And this algorithm makes virtual source points placed on an interior surface and is easier to implement than the boundary elements method since it does not require integrations over singular integrands.

Received 27 April 2008, revised 27 August 2008,
accepted 26 September 2008.

## 2. Theory of the wave superposition

An arbitrary-shaped vibrating structure with boundary is immersed in a homogeneous, compressible, and inviscid fluid. The geometry in the radiation problem is shown in Figure 1. The region enclosed by $S$ is denoted by $D$ and the region exterior to $S$ is denoted by $E$. A vector normal



© S. Hirzel Verlag · EAA

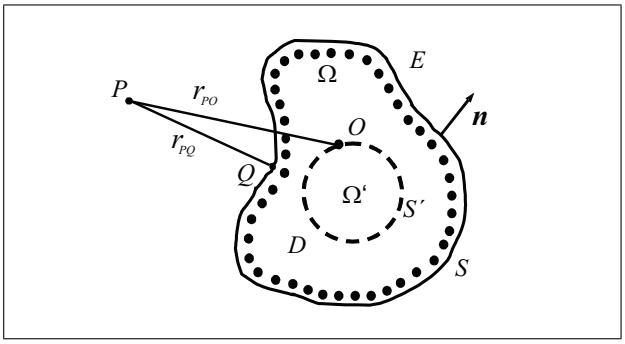



Figure 1. Geometrical description of vibrating structure.

to the surface $S$ pointing to the exterior region is shown as $\boldsymbol{n}$. $Q$ and $P$ are, respectively, any point of the surface $S$ and outer domain $E$. $r_{PQ}$ is the distance between $Q$ and $P$. We assume that virtual source points are continuous distributed in the internal domain $D$, and define the source surface $\Omega$ where virtual source points are placed.

From linear acoustic, the harmonic time dependence $\mathrm{e}^{-\mathrm{i}\omega t}$ is suppressed later, a monochromatic sound field is governed by the Helmholtz equation

$$\nabla^2 p + k^2 p = 0, \tag{1}$$

where $\nabla$ is the Laplacian operator, $p$ represents the complex amplitude of the pressure at any point $P$, $k = \omega/c = 2\pi/\lambda$ is the wave number, $c$ and $\lambda$ are the speed and wavelength of sound of the fluid medium, respectively. Satisfying the Sommerfeld radiation condition in the domain $E$ and the Neumann boundary condition in the boundary surface $S$, the acoustic radiation problem can be rewritten as

$$\begin{aligned} \nabla^2 p(\boldsymbol{r}) + k^2 p(\boldsymbol{r}) &= 0 \qquad \boldsymbol{r} \in E, \\ \boldsymbol{v}_n(\boldsymbol{r}) &= \overline{\boldsymbol{v}}_n(\boldsymbol{r}) \quad \boldsymbol{r} \in S, \\ \lim_{r\to\infty}\left[r\frac{\partial p(\boldsymbol{r})}{\partial r} + \mathrm{i}k p(\boldsymbol{r})\right] &= 0 \qquad \boldsymbol{r} \in E. \end{aligned} \tag{2}$$

According to the theory of wave superposition, the acoustic field radiated by an arbitrary-shaped vibrating structure can be substituted by a series of virtual source points located on a surface interior to the body of the radiator. The source strengths are determined by applying boundary conditions on the measurement surface. So the pressure in the outer domain $E$ may be written as

$$p(\boldsymbol{r}) = \mathrm{i}\rho\omega \int_\Omega q(\boldsymbol{r}_0) G(\boldsymbol{r}, \boldsymbol{r}_0)\, \mathrm{d}\Omega(\boldsymbol{r}_0), \tag{3}$$

where $\rho$ is the density of the fluid medium, $q(\boldsymbol{r}_0)$ is the source strength, $G$ is the Green function

$$G(\boldsymbol{r}, \boldsymbol{r}_0) = \frac{\mathrm{e}^{\mathrm{i}k|r-r_0|}}{4\pi|\boldsymbol{r} - \boldsymbol{r}_0|}. \tag{4}$$

Equation (5) is the theoretical formula of wave superposition when calculating acoustic radiation. The virtual source points can be placed any surfaces interior to the body of the radiator. But for simplifying calculation, the virtual source points are generally placed on a regular-shaped surface, such as sphere, ellipse and plane, etc. Here we choose spherical surface $\Omega'$, shown in Figure 1. $S'$ represents the boundary of the spherical surface $\Omega'$, and $O$ is the any point in the boundary $S'$. Since wave superposition method is accomplished by superposing wave fields generated by virtual source points interior to the radiator, there is no singular integration which is inherent to BEM-based NAH, and this is one of advantages of WSM-based acoustic holography.

Equation (5) can't be directly calculated. The boundary $S'$ should be discretized as $M$ regions, and the source strength is $Q(\boldsymbol{r}_i)$ in the region $i$. We define $N$ to be the number of measurement locations. Equation (5) may be rewritten in matrix form as

$$\boldsymbol{P} = \boldsymbol{G}_{q,h}\boldsymbol{q}, \tag{5}$$

where

$$\boldsymbol{q} = \begin{bmatrix} Q(\boldsymbol{r}_{S'1}) \\ \vdots \\ Q(\boldsymbol{r}_{S'M}) \end{bmatrix}, \tag{6}$$

$$\boldsymbol{P} = \begin{bmatrix} p(\boldsymbol{r}_{h1}) \\ \vdots \\ p(\boldsymbol{r}_{hN}) \end{bmatrix}, \tag{7}$$

$$\boldsymbol{G}_{q,h} = \begin{bmatrix} G(\boldsymbol{r}_{h1}, \boldsymbol{r}_{S'1}) & \cdots & G(\boldsymbol{r}_{h1}, \boldsymbol{r}_{S'M}) \\ \vdots & \ddots & \vdots \\ G(\boldsymbol{r}_{hN}, \boldsymbol{r}_{S'1}) & \cdots & G(\boldsymbol{r}_{hN}, \boldsymbol{r}_{S'M}) \end{bmatrix}, \tag{8}$$

where $\boldsymbol{q}$ is the column vector of virtual source points placed over the boundary surface $S'$, with size $M \times 1$. $\boldsymbol{G}_{q,h}$ is the project matrix from virtual source points $\boldsymbol{q}$ to measurement surface $h$, and has size $N \times M$. If matrix $\boldsymbol{G}_{q,h}$ can be inverted, the source strengths can be evaluated from the measured field values $\boldsymbol{P}$ using equation (5). Once the source strengths $\boldsymbol{q}$ are evaluated, any position of the outer domain $E$ can be reconstructed. Figure 2 shows the flow chart of the wave superposition method.

## 3. Data extrapolation

Data extrapolation based on patch near-field acoustic holography is to mitigate finite measurement aperture effects by allowing the sound field to be iteratively extended beyond the measurement aperture. As shown in Figure 3, the process of data extrapolation method is how to obtain the sound pressures $p_{h2}$ of extended surface $h_2$ using the sound pressures $p_{h1}$ of measurement surface $h_1$. This method enlarges equivalently the measurement surface, and can improve the reconstruction precision duo to mitigate the finite measurement aperture effects to the reconstruction result.

We define $N_{h1}$ and $N_{h2}$, respectively, to be the number of the measurement positions of holographic plane $h_1$ and $h_2$. And the extended plane $h_2$ includes $h_1$ in $z = z_h$.

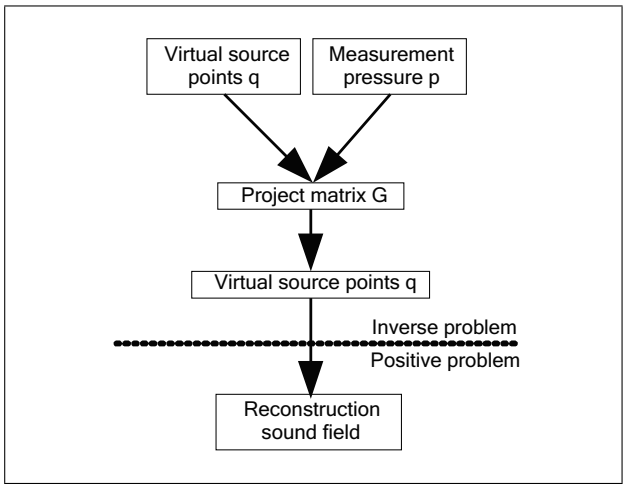



Figure 2. Flow diagram of WSM.

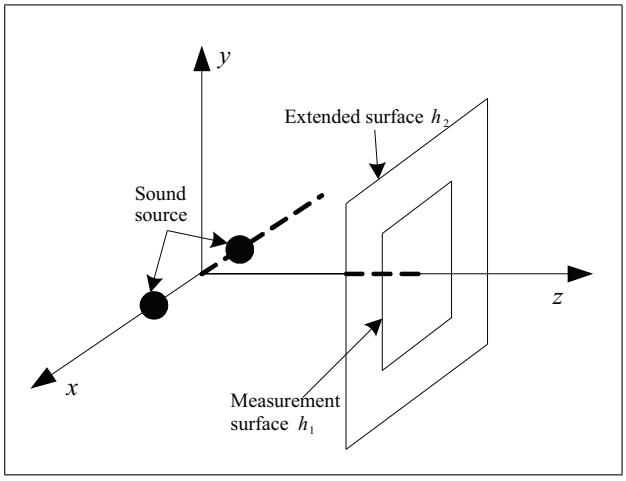



Figure 3. Data extrapolation.

Measurement location $j$ of surface $h_1$ has coordinates $r_{h1,j}$. Measurement location $i$ of surface $h_2$ has coordinates $r_{h2,i}$. $r_{s,j}$ represents the coordinates of virtual source point $q_j$. We next state data extrapolation method based on patch-NAH that the acoustic field is approximated by the field produced by $M$ sources placed on surface $S'$.

When the sound pressures $\boldsymbol{P}_{h_1}$ of the measurement surface $h_1$ are obtained, the source strengths can be determined by using equation(5). We invert matrix $\boldsymbol{G}_{q,h_1}$ and rewrite equation(5) as

$$\boldsymbol{q}^{(1)} = \boldsymbol{G}^{*}_{q,h_1}\boldsymbol{P}, \tag{9}$$

where matrix $\boldsymbol{G}^{*}_{q,h_1}$ is the generalized inverse of $\boldsymbol{G}_{q,h_1}$. Once the source strengths $\boldsymbol{q}^{(1)}$ are obtained using equation (9), the field of the surface $h_2$ may be approximated by

$$\boldsymbol{P}^{(1)}_{h_2} = \boldsymbol{G}_{q,h_2}\boldsymbol{q}^{(1)}. \tag{10}$$

In equation(10), $\boldsymbol{P}^{(1)}_{h_2}$ can be rewritten as

$$\boldsymbol{P}^{(1)}_{h_2} = \boldsymbol{P}_{h_1} + \boldsymbol{P}^{(1)}_{h_2-h_1}, \tag{11}$$

where $\boldsymbol{P}^{(1)}_{h_2-h_1}$ represents the sound pressure of region $h_2 - h_1$ which the extended surface $h_2$ subtracts the measurement surface $h_1$. Subsequently, the source strengths $\boldsymbol{q}^{(2)}$ can be obtained again using the sound pressures $\boldsymbol{P}^{(1)}_{h_2}$ and equation (5), then the sound pressure $\boldsymbol{P}^{(2)}_{h_2}$ and $\boldsymbol{P}^{(2)}_{h_2-h_1}$ of the extended surface $h_2$ can be determined using equations (10) and (11). After iterating $k$ times, we can obtain $\boldsymbol{P}^{(k)}_{h_2}$ and $\boldsymbol{P}^{(k)}_{h_2-h_1}$ until $||\boldsymbol{P}^{(k)}_{h_2-h_1} - \boldsymbol{P}^{(k-1)}_{h_2-h_1}||/\sqrt{M} <$ eps, where eps is the threshold value.

The threshold value eps plays an important role in the reconstruction precision. It means that the iteration procedure is stopped when there is minimal change in the update extended pressure, that is,

$$||\boldsymbol{P}^{(k)}_{h_2-h_1} - \boldsymbol{P}^{(k-1)}_{h_2-h_1}||/\sqrt{M} < \text{eps} = 0.1\sigma, \tag{12}$$

where the latter equality $\sigma$ is just the definition of the variance of the noise, and $||...||$ is the $L_2$ norm. This intuitive equation is attributed to Morozov and is called the Morozov discrepancy principle [18]. This equation reflects the fact that the minimal pressure change must depend on the noise level in the extended data. If eps is very small, it will increase the amount of calculation. On the contrary, if eps is very large, the iteration procedure cuts off too soon and the extrapolation is less accurate. The factor 0.1 worked well in most cases. However, we found it helpful to require a certain minimum number of iterations to take place before any cutoff criterion is applied. Unfortunately we cannot present proof that the iteration procedure presented above converges, but have found in all the test cases explored that it is robust and always converges as long as we use equation (13). We now use some examples to show the convergence of data extrapolation in numerical simulation.

It should be noticed that, in equation (9), if the number of measurement points is not equal to the number of virtual source points, $N_{h_1} \neq M$, matrix $\boldsymbol{G}_{q,h_1}$ will not be square and if $N_{h_1} < M$ (or $N_{h_2} < M$), the matrix $\boldsymbol{G}_{q,h_1}$ will be ill-conditioned. We thus use the Tikhonov regularization method to invert it. And the value of the regularization parameter at each iteration is determined based on use of the $L$-curve criteria.

In 1963, Tikhonov proposed a regularization method to solve the ill-posed problem in his creative work [19]. Let $f_i = \lambda_i^2/(\lambda_i^2 + \alpha^2)$ be the regularization filter factors. So the regularized solution of equation (9) can be written as

$$\boldsymbol{q}_{\text{Reg}} = \sum_{i=1}^{n} f_i \frac{u_i^T p}{\lambda_i}\boldsymbol{v}_i = \sum_{i=1}^{n} \frac{\lambda_i^2}{\lambda_i^2 + \alpha^2}\frac{u_i^T p}{\lambda_i}\boldsymbol{v}_i, \tag{13}$$

where $\alpha$ is the regularization parameter. This parameter is important for the reason that it controls the degree, to which the small singular values are filtered. A larger $\alpha$ will cause over regularization; on the contrary, a smaller $\alpha$ will cause under regularization. So there exists an optimal parameter $\alpha$. There are many methods to determine the regularization parameter $\alpha$. Among these methods, $L$-curve

criteria uses the logarithmic scale to describe the regularized solution $||q_{\mathrm{Reg}}||_2$ and residual norm $||Gq_{\mathrm{Reg}}-p||_2$, then compare the results to determine the regularization parameter. Because the result map will obviously appear an $L$-curve shape, so called the L-curve criteria.

For the data extrapolation method based on patch-NAH, the location of virtual source surface and the number of virtual source points make great influence on the reconstruction results. According to the reference [13], Koopmann *et al.*, recommend that the ratio of virtual source surface and radiator's surface is between 0.05 and 0.5. Some authors [20], on the other hand, have shown that the ratio should be about 0.5. Here, the ratio in the simulation and experiment is set into 0.5. The number of virtual source points is determined based on the following reasons, (1) the number of virtual source points is less than the number of microphones in order to treat the discrete ill-posed problem in equation (9); (2) all virtual source points are uniformly collocated on the virtual source surface, so the angle of two neighbouring virtual source points in longitudinal direction(or latitudinal direction) is a fixed value since the virtual source surface is a spherical surface; (3) under satisfying the conditions (1) and (2), the number of virtual source points is increased to the greatest degree because the reconstruction precision is improved with increasing the virtual source points. Table.1 shows the comparisons of the number of measurement points and virtual source points.

As mentioned above, we can use equations (9) and (12) to realize the data extrapolation from the measurement surface $h_1$ to the extended surface $h_2$. The procedure of data extrapolation based on patch-NAH is briefly described as follows:

**Step.0:** the source strengths $\boldsymbol{q}^{(1)}$ are obtained using the sound pressures $\boldsymbol{P}_{h_1}$ of measurement surfaceand equation (9).

**Step.1:** the sound pressures $\boldsymbol{P}_{h_2}$ of extended surface $h_2$ are determined by $\boldsymbol{q}^{(1)}$ and equation (10).

**Step.2:** The sound pressures $\boldsymbol{P}_{h_2}$ of overlapping region between $h_1$ and $h_2$ is substituted by the sound pressures $\boldsymbol{P}_{h_1}$, $\boldsymbol{P}^{(1)}_{h_2} = \boldsymbol{P}_{h_1} + \boldsymbol{P}^{(1)}_{h_2-h_1}$.

**Step.3:** the source strengths $\boldsymbol{q}^{(2)}$ are obtained using the sound pressures $\boldsymbol{P}^{(1)}_{h_2}$ of the extended surface $h_2$ and equation (5).

**Step.4:** the sound pressures $\boldsymbol{P}_{h_2}$ of surface $h_2$ are determined by equation (10) and $\boldsymbol{q}^{(2)}$, then return to step.2.

**Step.5:** After iterating $k$ times, we can obtain $\boldsymbol{P}^{(k)}_{h_2} = \boldsymbol{P}_{h_1} + \boldsymbol{P}^{(k)}_{h_2-h_1}$.

**Step.6:** if $\boldsymbol{P}^{(k)}_{h_2-h_1} - \boldsymbol{P}^{(k-1)}_{h_2-h_1} <$ eps, iteration is over. Otherwise, return to step.3.

**Step 7:** the sound field of reconstruction surface is obtained using equations (9) and (10).

## 4. Numerical simulation

To verify the data extrapolation method based on patch-NAH, a simulation experiment is done with two ball sound sources, with vibration frequency 500 Hz. Two ball sound sources are placed on (−0.5 m, 0, 0) and (0.5 m, 0, 0), and the radius is 0.1 m. The sound velocity is 340 m/s. The measurement surface $h_1$ contains a 11 × 11 grid of points on the $z_h = 0.5$ m. The extended surface $h_2$ contains a 11 × 11 grid of points at the same position. The reconstruction is performed at a 15 × 15 grid of points again, on the surface $z_r = 0.1$ m. The interval of the holography surface and reconstruction surface is 0.1 m. Obviously, the measurement condition does not satisfy if using near-field acoustical holography.

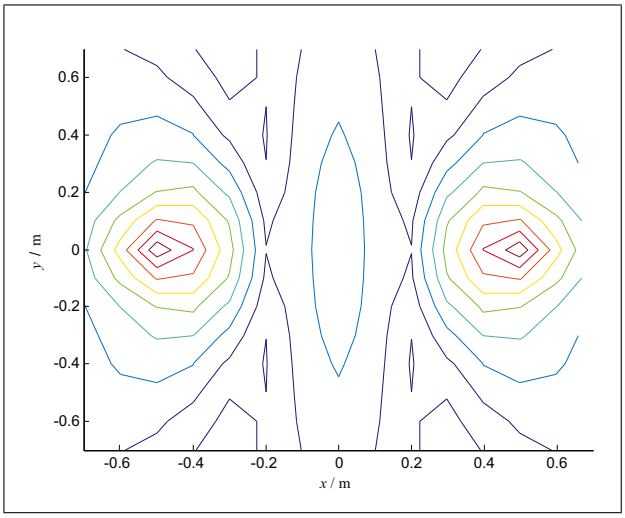



Figure 4. Contour map of theoretical sound pressure.

To the computed field values $\boldsymbol{P}_{h_1}$, we add background noise (SNR = 30 dB) to obtain

$$\tilde{\boldsymbol{P}}_{h_1} = \boldsymbol{P}_{h_1} + E_{\mathrm{noise}}, \tag{14}$$

where $E_{\mathrm{noise}}$ is the noise and the relative errors are defined as

$$\mathrm{err}(i) = \frac{|p^{\mathrm{true}}(i) - p_r(i)|}{|p^{\mathrm{true}}(i)|} \times 100, \tag{15}$$

where $p_r(i)$ represents the reconstruction pressure, and $p^{\mathrm{true}}(i)$ is the theoretical pressure.

Figure 4 shows the contour map of sound pressures in reconstructed surface obtained by theoretical formula. It can be seen that two sound sources locate at (−0.5 m, 0, 0) and (0.5 m, 0, 0), respectively.

In Figure 5, the sound pressure of reconstructed surface is calculated, directly, using the measurement pressure $\boldsymbol{P}_{h_1}$ of the measurement surface $h_1$. The position of two sound sources can be identified (see Figure 5,right). However, the relative errors are large and the maximum value reaches to 27%. And the errors of the edge areas are larger than those of the centre areas, where the maximum value is nearly 15%. The reason leading to this result is that the holography surface is smaller than the reconstructed surface.

According to the principle of section 3, in the first iteration, the number of virtual source points is 84 in order

Table I. The number of virtual source points with different measurement surface.

| The number of measurement points | 5 × 5 | 7 × 7 | 9 × 9 | 11 × 11 | 13 × 13 | 15 × 15 |
|---|---|---|---|---|---|---|
| The number of virtual source points | 14 | 30 | 54 | 84 | 126 | 172 |

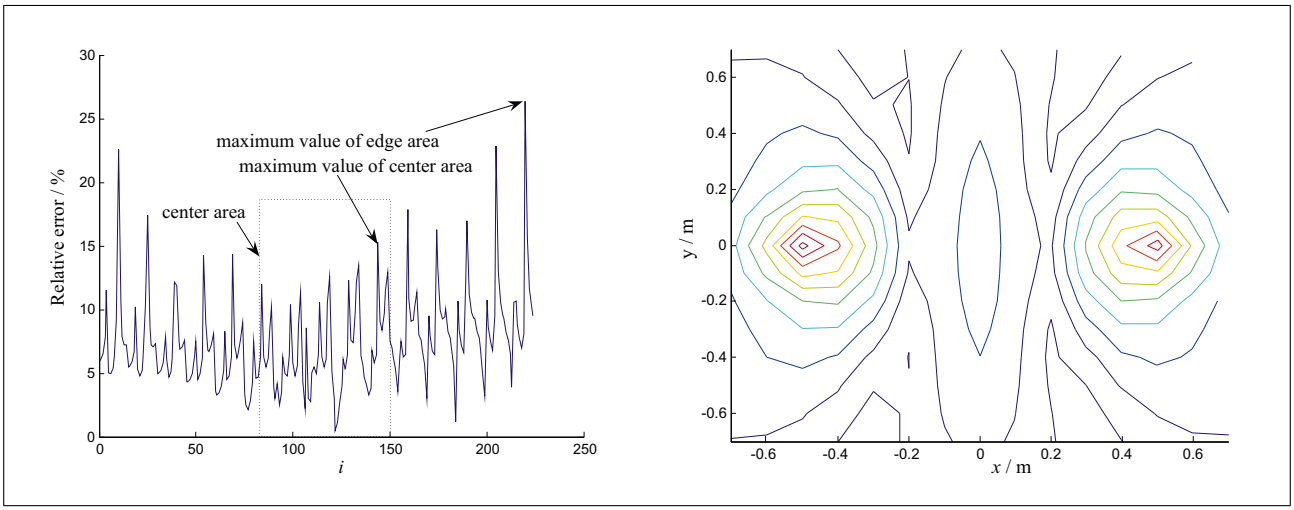



Figure 5. Reconstruction sound pressure without data extrapolation method: (left) relative errors; (right) contour map.

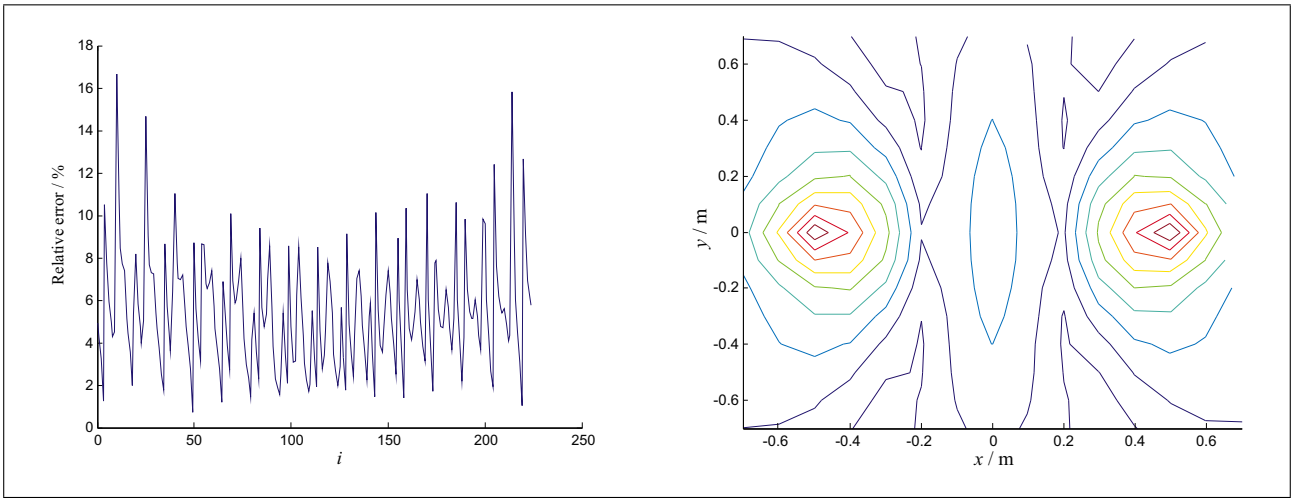



Figure 6. Reconstruction sound pressure using data extrapolation method with iterating one time and 172 virtual source points: (left) relative errors; (right) contour map.

to ensure that it is smaller than the number of the measurement points of holography surface $h_1$, 11 × 11. Once the sound pressures of extended surface $h_2$ are obtained, the number of virtual source points is changed to be 172 when using equation (10), because the extended surface is 15 × 15. Figures 6, 7, 8 show the result with changing the number of the virtual source points, and Figure 9 shows the result without changing the number of virtual source points after iterating three times.

Figures 6, 7, 8 show the relative errors and contour map of the reconstruction pressures after iterating one, two, three times, respectively. We find that beyond a certain number of iterations (as shown in Figure 10), the rate of error decrease slowed and only a very slight degree of continuing improvement is observed. It can be seen that the relative errors are gradually decreased with the increase of the number of the iteration. The maximum value of Figure 6, 7, 8 is 17%, 15%, 7.5%, respectively. They are obviously reduced compared with Figure 5, 27%, which does not use the data extrapolation method.

Compared Figure 8 with Figure 9, we find that the relative errors are obviously reduced when changing the number of virtual source points. In Figure 9, the maximum value of relative errors reaches to 15% after iterating three times, larger than 7.5% in Figure 8. But it is smaller than 27% in Figure 5.

In order to explain the convergence of data extrapolation, Figure 10 shows the comparison of the reconstruction

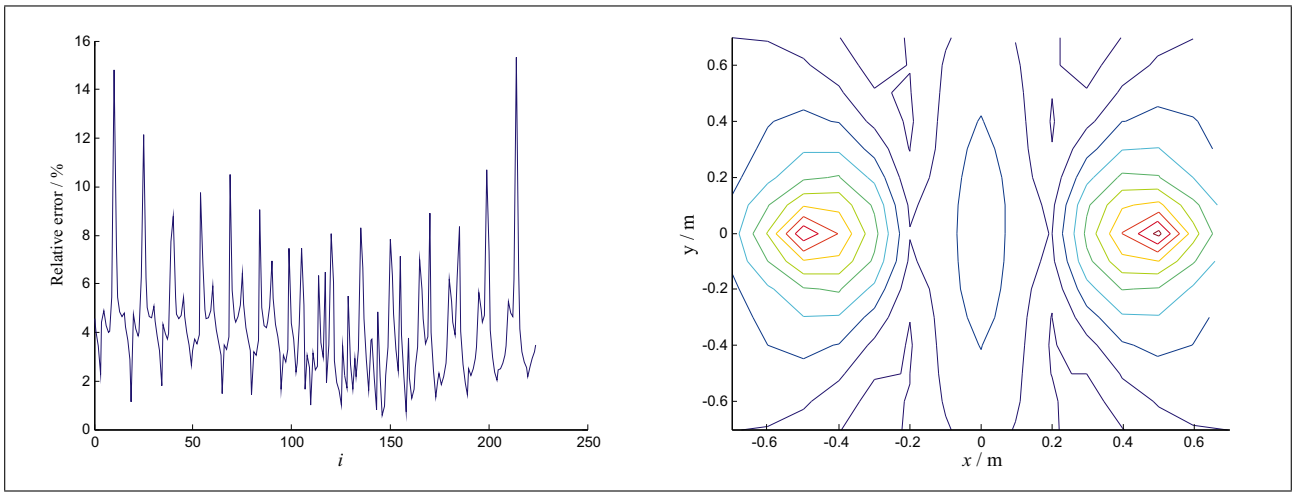



Figure 7. Reconstruction sound pressure using data extrapolation method with iterating two times and 172 virtual source points: (left) relative errors; (right) contour map.

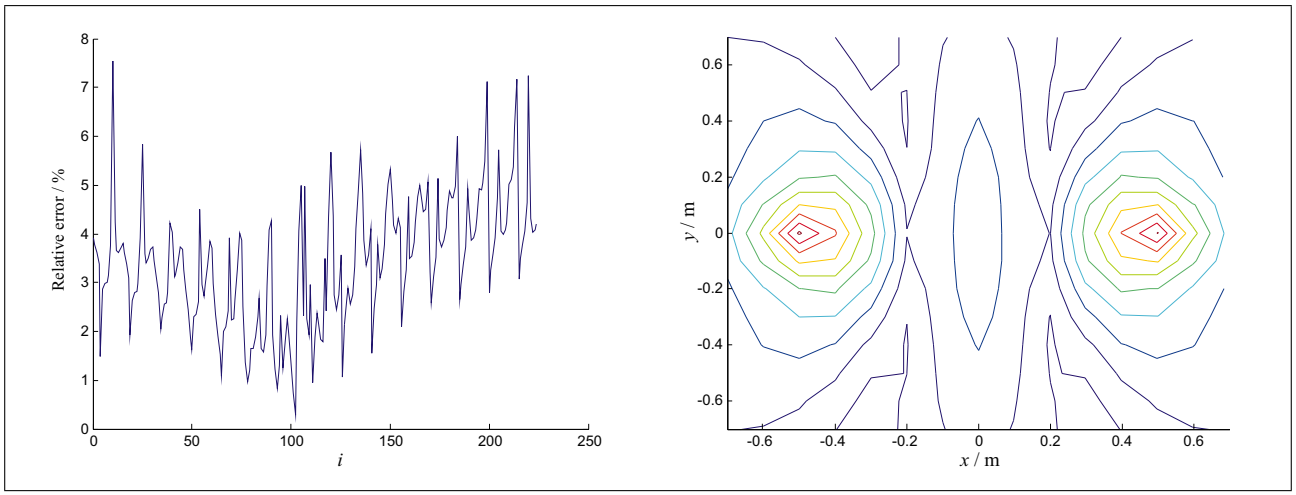



Figure 8. Reconstruction sound pressure using data extrapolation method with iterating three times and 172 virtual source points: (left) relative errors; (right) contour map.

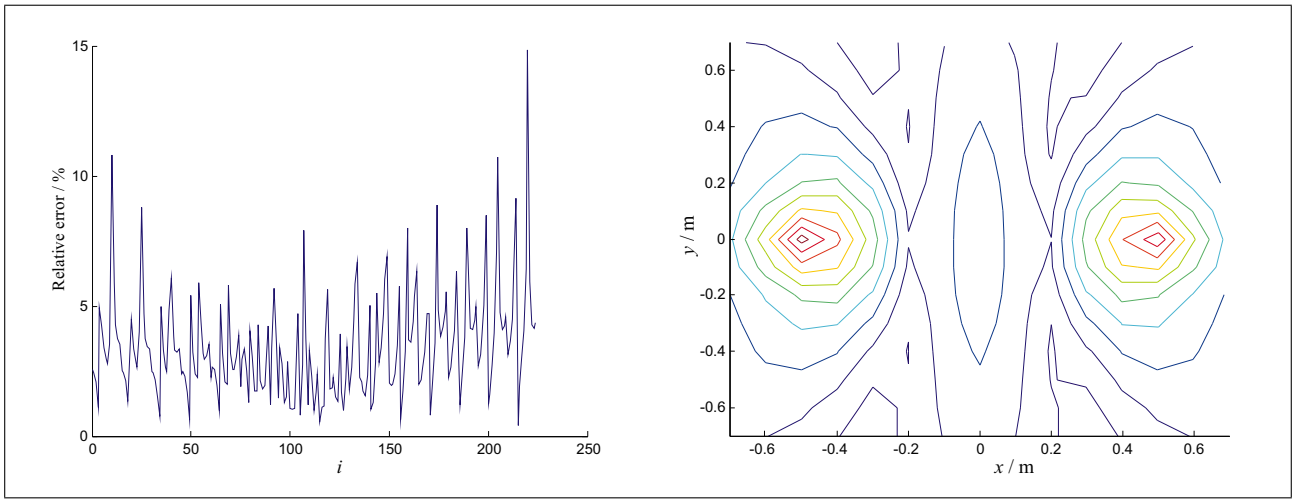



Figure 9. Reconstruction sound pressure using data extrapolation method with iterating three times and 84 virtual source points: (left) relative errors; (right) contour map.

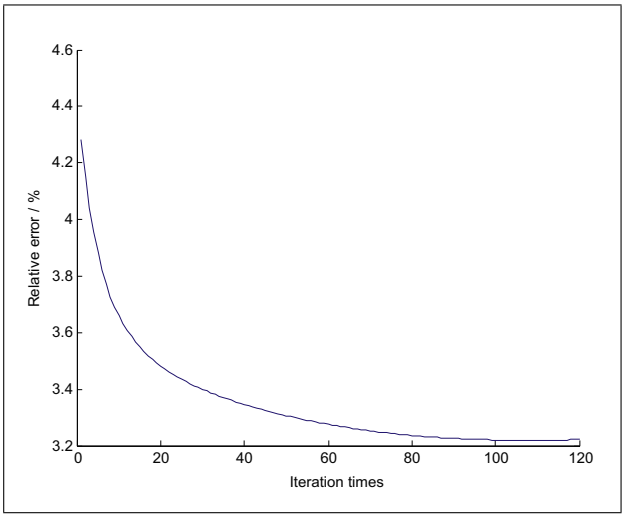



Figure 10. Comparison of the reconstruction errors with different iterative times.

errors with 172 virtual source points and different iterative times. In this figure, we can find that the reconstruction errors gradually decease with the increase of iterative times. The global error is 4.3% in the first iteration, however, it reduces to 3.2% after iterating 120 times. And the rate of error decrease slowed and only a very slight degree of continuing improvement is observed after iterating 80 times. Figure 10 also shows that the error tends to a stable value, and can prove that the data extrapolation based on patch-NAH is convergent.

## 5. Experimental validation

Besides simulation experiment, a experiment research is done in a semi-anechoic chamber, whose dimensions are $7 \times 4.5 \times 4.3\,\mathrm{m}^3$. The experimental test setup is shown in Figure 11a. The sound sources are set up as two high fidelity loudspeakers whose positions are placed at (0, 0, 0) and (−0.4 m, 0, 0). A holography surface consisting of 25 microphones is placed to measure sound signals. Its size is $0.4 \times 0.4\,\mathrm{m}^2$ and the interval between neighboring microphones is 0.1 mm. The distance between the holography surface and the two sound sources is 0.1 m. The extended surface is as same as the holography surface except that its size is $1.2 \times 1.2\,\mathrm{m}^2$ and includes a 13 × 13 grid of points (shown in Figure 11b). The reconstruction is performed at $z_r = 0.05\,\mathrm{m}$ and the reconstruction surface is the same as the extended surface.

Figure 12 shows the contour map of sound pressures in the holography surface. It can be seen that one sound source is placed at (0, 0, 0), and there is another sound source in its left. However the accurate position of the second sound source can not be obtained.

In order to compare the difference of varying the number of virtual source points, the reconstructed sound pressures are obtain using 14 and 126 virtual source points. Based on the method of determining the number of virtual source points, in the first iterative calculation, the number

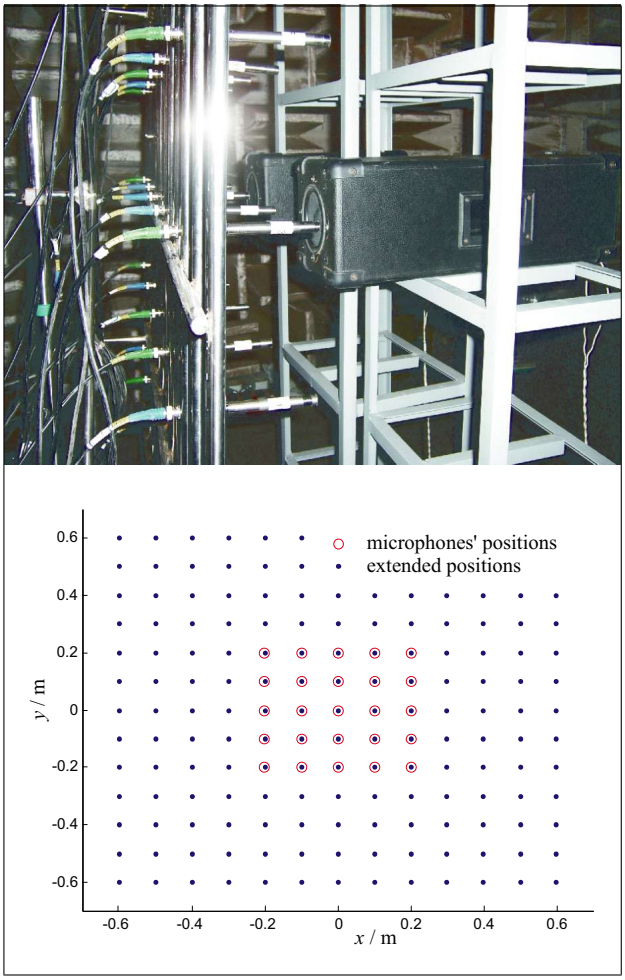



Figure 11. Top: Experimental test setup of two sound sources; bottom: array distribution map of microphone's positions and extended positions.

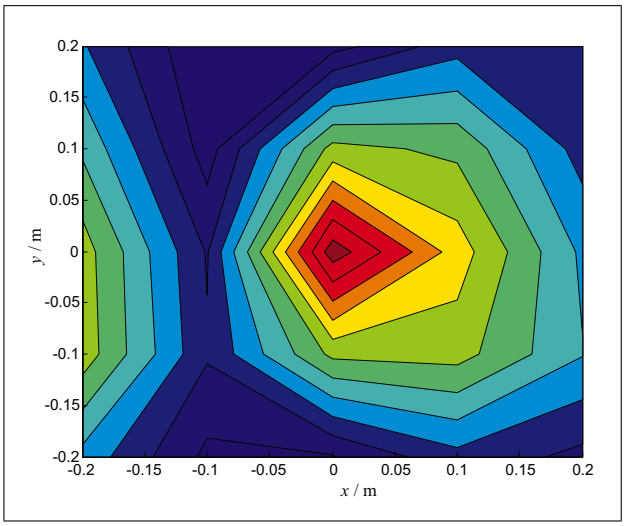



Figure 12. Contour map of measurement sound pressure.

of virtual source points is 14, since the number of measurement points of holography surface is 25. After completing

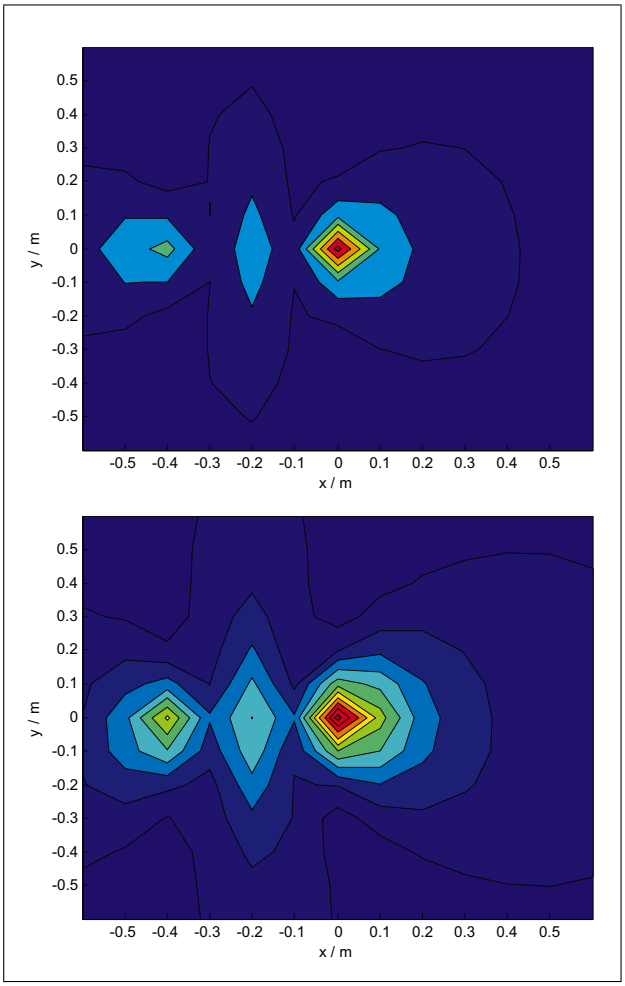



Figure 13. Reconstruction sound pressure using data extrapolation method with iterating four times. Top: 14 virtual source points; bottom: 126 virtual source points.

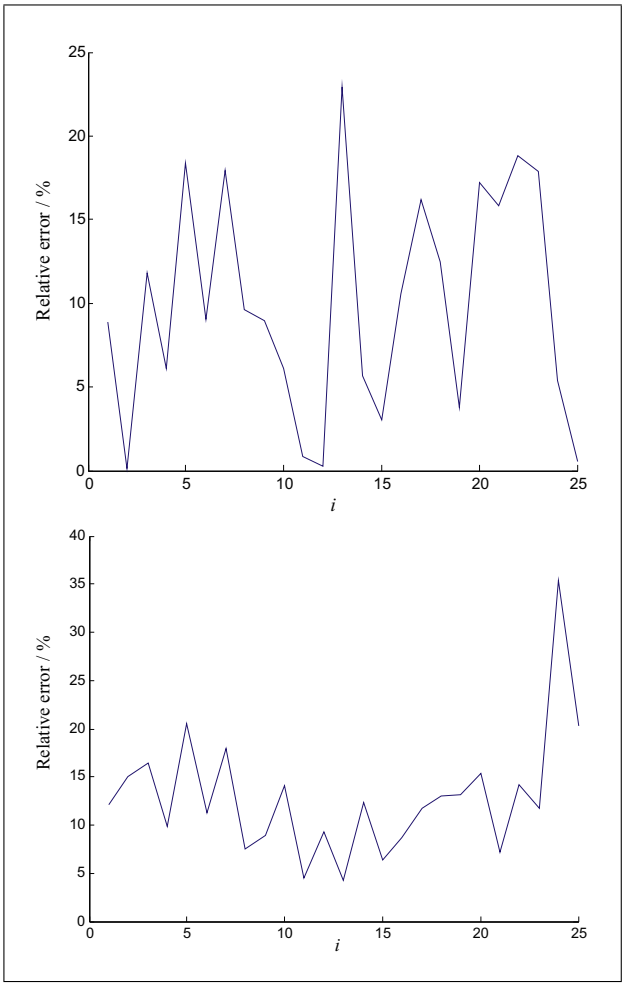



Figure 14. Relative errors of reconstruction sound pressure. Top: with data extrapolation method; bottom: without data extrapolation method.

the first iteration, it changes to 126, because the extend measurement points are 169.

After iterating four times, the reconstruction sound pressures without changing the number of virtual source points are presented in Figure 13,top. In that figure, the main sound source can be identified, and it located at (0, 0, 0). However, it will be doubted that there is another sound source at (−0.4 m, 0, 0), since it is not significant. When the number of virtual source points is changed to 126 after iterating one time, Figure 13,bottom shows the reconstruction sound pressures after iterating four times. We can clearly see that two sound source are placed at (−0.4 m, 0, 0) and (0, 0, 0), respectively.

In order to determine the reconstructed errors, the reconstruction surface is placed at $z_r = 0.1$ m. And we compare the reconstructed sound pressures with measurement sound pressures. Figure 14,top shows the relative errors of reconstructed sound pressure when using data extrapolation method, and Figure 14,bottom presents the relative errors of reconstructed sound pressure without data extrapolation method. By comparing both parts of Figure 14, it can be found that the maximum error is less than 25% in Figure 14,top when using data extrapolation method. However, the maximum value of Figure 14,bottom reaches to 35% without data extrapolation method. And the error is decreased by 10%. Therefore, the influence of finite measurement surface on the reconstructed results, to some extent, has been restrained by using the proposed data extrapolation method. So the results of simulation and experiment show the superiority of the data extrapolation method based on patch-NAH, and demonstrate its validity and applicability.

## 6. Conclusions

In the conventional NAH, the reconstruction error is inevitable because of the finiteness of measurement aperture. It means that such a deficiency requires the measurement surface sufficiently larger than the vibrating object for conventional NAH. This prevents conventional NAH from being applied to an actual large-scale structure. In order to remove the influence of the finiteness of measurement surface, the data extrapolation method based on patch-NAH has been proposed. However, we cannot present the proof that the data extrapolation method is convergent, but have found that it is robust and always converges to a sta-

ble value. The validity of the proposed data extrapolation method is demonstrated by numerical simulation and experiment. The results show that the method may be applied to reconstruct the acoustic field in regions located near to the measurement surface, and the errors are reduced significantly when the extended pressures are used. The algorithm is very easy to implement either to flat or curved surfaces. It may be used to extrapolate the field outward to enlarge the measurement surface in order to improve the reconstructed precision.

**Acknowledgement**

This work was supported by National Natural Science Foundation of China, Project NO.50675140.

**References**

[1] E. G. Williams, J. D. Maynard: Holographic imaging without the wavelength resolution limit. Physical Review Letter **45** (1980) 554–557.

[2] E. G. Williams: Sound source constructions using a microphone array. Journal of the Acoustical Society of America **68** (1980) 340–344.

[3] J. D. Maynard, E. G. Williams, Y. Lee: Near-field acoustic holography: Theory of generalized holography and the development of NAH. Journal of the Acoustical Society of America **78** (1985) 1395–1413.

[4] W. A. Veronesi, J. D. Maynard: Digital holographic reconstruction of sources with arbitrarily shaped surfaces. Journal of the Acoustical Society of America **85** (1989) 588–598.

[5] G. V. Borgiotti, A. Sarkissian, E. G. Williams, L. Schuetz: Conformal generalized near-field acoustic holography for axisymmetric geometries. Journal of the Acoustical Society of America **88** (1990) 199–209.

[6] A. Sarkissian: Near-field acoustic holography for an axisymmetric geometry: a new formulation. Journal of the Acoustical Society of America **88** (1990) 961–6.

[7] E. G. Williams: Regularization methods for near-field acoustical holography. Journal of the Acoustical Society of America **110** (200) 1976–1988.

[8] E. G. Williams, B. H. Houston, P. C. Herdic: Fast Fourier Transform and singular value decomposition formulations for patch near-field acoustical holography. Journal of the Acoustical Society of America **114** (2003) 1322–1333.

[9] K. Saijyou, S. Yoshikawa: Reduction methods of the reconstruction error for large-scale implementation of near-field acoustical holography. Journal of the Acoustical Society of America **110** (2001) 2007–2023.

[10] E. G. Williams: Continuation of acoustic near-fields. Journal of the Acoustical Society of America **113** (2003) 1273–1281.

[11] K. Saijyou: Regularization method for the application of k-space data extrapolation to near-field acoustical holography. Journal of the Acoustical Society of America **116** (2004) 396–404.

[12] K. Saijyou, H. Uchida: Data extrapolation method for boundary element method-based near-field acoustical holography. Journal of the Acoustical Society of America **115** (2004) 785–796.

[13] G. H. Koopmann, L. Song, J. B. Fahnline: A method for computing acoustic fields based on the principle of wave superposition. Journal of the Acoustical Society of America **86** (1989) 2433–2438.

[14] A. Sarkissian: Extension of measurement surface in near-field acoustic holography. Journal of the Acoustical Society of America **115** (2004) 1593–1596.

[15] W. F. Xue, J. Chen, G. C. Zhang: Sound sources identification for machine acoustic signals based on combined wave superposition method. Acta Acustica united with Acustica **92** (2006) 45–50.

[16] A. Sarkissian: Method of superposition applied to patch near-field acoustic holography. Journal of the Acoustical Society of America **118** (2005) 671–678.

[17] N. P. Valdivia, E. G. Williams: Study of the comparison of the methods of equivalent sources and boundary element methods for near-field acoustic holography. Journal of the Acoustical Society of America **120** (2006) 3694–705.

[18] V. A. Morozov: Choice of parameter for the solution of functional equation by the regularization method. Journal of Soviet Mathematics Doklady **8** (1967) 1000–1003.

[19] A. N. Tikhonov, V. Y. Arsenin: Solutions of ill-posed problem. John Wiley and Sons, New York, 1977.

[20] L. Song, G. H. Koopmann, J. B. Fahnline: Numerical errors associated with the method of superposition for computing acoustic fields. Journal of the Acoustical Society of America **89** (1991) 2625–2633.